Int. J. Pharm. Investigation, 2026; 16(3):1123-1134.
https://www.jpionline.org

Original Article

Design and Optimization of Arginine-Loaded Nutraceutical Nanoparticles via Face-Centered Central Composite Approach

Vijay Sharma[1,*], Maneesh Kumar Singh[2], Gurvinder Pal Singh[3], Gyanendra Kumar Sharma[3], Navneet Verma[1]

[1]Pharmacy Academy, Faculty of Pharmacy, IFTM University, Moradabad, Uttar Pradesh, INDIA.
[2]Departemt of Pharmaceutics, IIMT University, Meerut, Uttar Pradesh, INDIA.
[3]Sharda School of Pharmacy, Sharda University Agra, Agra, Uttar Pradesh, INDIA.

ABSTRACT

Aim/Background: The aim of the present study was to develop and optimize a dosage form of L-arginine as a nanoparticle for prolonged release. The Quality by Design (QbD) approach was employed to develop and optimize the dosage form using Face Centered Central Composite Design (FCCCD). Nutraceutical-loaded nanoparticles were developed by nanoprecipitation technique using Eudragit L 100, methanol and polyvinyl alcohol solution. **Materials and Methods:** The concentration of Eudragit L 100 and solvent to antisolvent was considered as independent variable whereas particle size, zeta potential, drug loading and entrapment efficiency were the dependent responses. A 3^2 FCCCD was used to develop 3D Response surface plot and to get an optimized formulation. **Results:** The optimized formulation demonstrated desirable values of Particle Size of 103.97 nm, Zeta Potential of 0.771, Drug Loading (%) of 24.826, and Entrapment Efficiency (%) 74.26. The optimized formulation was validated by preparing four additional batches using the determined optimal values of independent variables. A comparison between the experimental and predicted values demonstrated close agreement, confirming the reliability of the optimized data. **Conclusion:** The current research study helps to optimize L-arginine drug delivery systems, significantly reducing the need for exhaustive experimentation while ensuring high-quality formulations.

Keywords: Eudragit L 100, L-arginine, Quality by design, Response Surface methodology, Validation check.

Correspondence:
Dr. Vijay Sharma
Professor, Pharmacy Academy, Faculty of Pharmacy, IFTM University, Moradabad, 244102, Uttar Pradesh, INDIA.
Email: vijaysrampur@gmail.com

Received: 08-01-2026;
Revised: 16-03-2026;
Accepted: 21-05-2026.

INTRODUCTION

Nanoparticles are the primary nanoparticulate drug delivery systems, offering significant advantages for targeted drug delivery and improving the dissolution rate and bioavailability of poorly water-soluble drugs. The development of drug-loaded nanoparticles is a highly promising strategy. Various techniques are available to reduce particle size to the nanometer scale, and these methods have been extensively studied. The poor solubility and low dissolution rate of Biopharmaceutical Classification System (BCS) Class II drugs in aqueous gastrointestinal fluids often lead to inadequate bioavailability. Enhancing solubility and dissolution rate through advanced techniques is essential to overcoming this limitation. Several approaches, such as solid dispersion, inclusion complex formation, and the use of microparticles and nanoparticles, have been employed to improve drug dissolution rates (Rizvi and Saleh, 2021; Bhalani *et al*., 2022).

The nanoprecipitation technique, also known as the solvent displacement method, is a simple, rapid, and efficient approach to nanoparticle formulation. It involves the precipitation of a preformed polymer from an organic solution, followed by the diffusion of the organic solvent into an aqueous medium, with or without the presence of a surfactant. This method requires two mutually miscible solvents, where both the polymer and the drug should be soluble in one solvent but insoluble in the other (non-solvent) (Bhalani *et al*., 2055). Nanoprecipitation occurs through rapid desolvation of the polymer when the polymer solution is introduced into the aqueous phase. As the organic solvent diffuses into the aqueous medium, the polymer precipitates, leading to the immediate entrapment of the drug. Polymer deposition at the interface of the aqueous and organic phases, driven by rapid solvent diffusion, results in the spontaneous formation of a colloidal suspension. This technique is particularly suitable for hydrophobic compounds that are

DOI: 10.5530/ijpi.20260567

soluble in ethanol or acetone but exhibit minimal solubility in water (Beck-Broichsitter *et al.*, 2010).

Arginine, or L-arginine, is a semi-essential amino acid involved in various physiological processes. It plays a key role in protein synthesis, immune function, and wound healing. Arginine is a precursor for Nitric Oxide (NO), a vital molecule that regulates blood vessel dilation, improving circulation and cardiovascular health. It also contributes to ammonia detoxification through the urea cycle and enhances hormone secretion, including insulin and growth hormone (Salatin *et al.*, 2017). The Central Composite Design (CCD) enables systematic optimization of arginine-loaded nanoparticles by assessing the impact of key formulation variables. It ensures maximum drug entrapment, controlled release, and enhanced bioavailabilitywhile minimizing experimental runs. CCD improves formulation efficiency, making the process cost-effective, reproducible, and scalable. This approach enhances nanoparticle performance for nutraceutical and pharmaceutical applications (Wu *et al.*, 2009).

MATERIALS AND METHODS

L-arginine was obtained from CDH Laboratory Chemicals, Eudragit L-100 was purchased from BFC Laboratories, Banglore, India, poly vinyl alcohol, methanol and acetone were purchased from Molychem, (Mumbai, India). All other materials or chemicals used were of analytical grade.

Preparation of nanoparticles

Arginine-loaded nanoparticles were formulated using the nanoprecipitation technique with varying polymer concentrations, optimized through a 3^2 Face-Centered Central Composite Design (FCCCD) (Table 1). Eudragit L100 was dissolved in methanol, while arginine was dissolved in acetone, and the two solutions were mixed. The resulting mixture was added dropwise into an aqueous polyvinyl alcohol solution under stirring at 700 rpm for 120 min. After completing organic solvent evaporation, the dispersion was centrifuged at 13,000 rpm, and the collected nanoparticles were dried at 40°C for 1 hr to obtain the final product (Becker *et al.*, 1967).

Designing of experiment

A Face centered 3^2 Central Composite Design (FCCCD) was employed for the optimization study, focusing on two independent variables: Eudragit L100 concentration (X1) and solvent: antisolvent ratio (X2). Their effects were evaluated on key dependent responses, including Particle Size (nm), average zeta Potential (mV), Drug Loading (%), and Entrapment Efficiency (%). The experimental design points are detailed in Table 1.

Polynomial equations were formulated to describe the relationship between independent and dependent variables. The general polynomial equation used to assess these effects is:

$$Y1=b_0+b_1X_1+b_2X_2+b_3X_1X_2+b_4X_1^2+b_5X_2^2+b_6X_1X_2^2+b_7X_1^2X_2$$

where Y1 represents the dependent response, and b0 is the arithmetic mean response across 13experimental runs. This statistical approach allows for efficient optimization and evaluation of nanoparticle formulation parameters (López-Ruiz *et al.*, 2022).

Characterization of nanoparticles

Particle size analysis

The mean particle size of nanoparticles was determined using the Malvern instrument (ver. 6.12). The analysis was conducted by introducing 0.3 mL of the sample into the viewing unit, where Dynamic Light Scattering (DLS) was utilized to measure both particle size and molecular size. The measurements were taken at a scattering angle of 90° at room temperature. The particle size was recorded as the mean±standard deviation, based on three parallel measurements. This technique estimates particle size distribution by analyzing Brownian motion and converting the diffusion data into size parameters (Sadhukhan *et al.*, 2016).

Zeta potential measurement

The zeta potential analysis was conducted using the Malvern Zeta sizer (ver. 6.12, Malvern Instruments, UK). The electrophoretic mobility of the nano particles was measured and converted into zeta potential. For the analysis, the nano particle samples were diluted with 0.1 mM KCl and placed in an electrophoretic cell, where an electric field of 15.2 V/cm was applied. All measurements were performed in triplicate to ensure accuracy and reproducibility (Stetefeld *et al.*, 2016).

Percent drug loading and entrapment efficiency

A precisely weighed sample of 10 mg drug-loaded nanoparticles was dispersed in 10 mL of dichloromethane and subjected to sonication for 1 hr. The resulting solution was then filtered using a membrane filter and analyzed using HPLC with UV detector (Carissimi *et al.*, 2020). The drug loading percentage and Entrapment Efficiency (EE) were calculated using the following formulas:

$$\text{Drug Loading (\%)} = \frac{\text{Mass of drug in nanoparticles}}{\text{Mass of nanoparticles recovered)}} \text{ X } 100$$

$$\text{Entrapment Efficciency} = \frac{\text{Mass of drug in nanoparticles}}{\text{Mass of drug used in preparation}} \text{ X } 100$$

To ensure precision and reproducibility, all measurements were conducted in triplicate.

Scanning Electron Microscopy (SEM)

The nanoparticles were subjected to gold-palladium coating using a sputter coater unit (VG-Microtech, UK) to enhance conductivity. The surface morphology was then analyzed using a Cambridge Stereoscan S120 Scanning Electron Microscope

(SEM, Cambridge, UK), operated at an acceleration voltage of 10 kV (Goldstein *et al.*, 2014).

In vitro drug release studies

For the drug release study, nanoparticles were enclosed in dialysis bags, securely sealed, and immersed in a Phosphate Buffer (pH 6.8) containing 1% sodium lauryl sulfate. The dissolution process was carried out using a USP Type II apparatus, set at 37±0.5°C with a stirring speed of 100 rpm for 2 hr. At designated time intervals, 5 mL of the medium was withdrawn and replaced with fresh buffer to maintain sink conditions. The withdrawn samples were then filtered using Whatman filter No. 41, appropriately diluted, and analyzed using a UV-vis spectrophotometer (Mast *et al.*, 2021).

Factorial design/statistical analysis

Experimental design with a coded level of variables and their actual values are illustrated as the effects of the different concentrations of drug and polymer ratio (X1), the concentration of surfactant (X2) and the ratio of organic solvents (X3) on the responses.

Optimization and data validation

Eudragit L 100 concentrations were varied at 4 mg, 5 mg, and 6 mg, while the solvent-to-antisolvent ratio was adjusted to 1:3, 1:4, and 1:5. A total of thirteen formulations were designed, incorporating nine different combinations, with the centre point replicated four times, and the average value was considered for further evaluation. The dependent responses were analysed using Design Expert® 8.0.7.1 (trial version), and statistical models were assessed for significance. The optimised formulation was selected based on the desired dependent response values. Additionally, four formulations (VC1 to VC4) were developed alongside the optimized batch and validated using response surface methodology. The predicted and observed responses were critically compared using linear correlation plots. Residual graphs depicting the differences between predicted and observed values were generated, and the percent prediction error (% bias) was determined. A total of four formulations were selected as checkpoints to validate the optimized formulation (Tian *et al.*, 2018).

RESULTS

Visual inspection of the L-Arginine sample revealed it to be a white, crystalline powder. The melting point of the sample was observed to be 228°C, which lies within the reported range of 222-233°C, confirming the expected physical characteristics of the compound.

The FTIR (Fourier Transform Infrared) spectrum of the formulated L-arginine nanoparticles was recorded to evaluate potential drug-polymer interactions. The infrared spectra of both the pure drug and the nanoparticle formulation exhibited similar characteristic peaks, as shown in Table 2 and Figures 1 and 2.

Formulation Optimization Using Central Composite Design (CCD)

A 3^2 Central Composite Design (CCD) was employed for the systematic optimization of Nanoparticles of L-Arginine (ARG), as shown in Tables 1. A total of thirteen experimental batches were formulated based on the CCD matrix. The data obtained were fitted to a second-order quadratic polynomial model using Multiple Linear Regression Analysis (MLRA).

The MLRA yielded mathematical models for key Critical Quality Attributes (CQAs) such as particle size, zeta potential, drug loading, and entrapment efficiency. The high correlation coefficients (R^2 values ranging from 0.9497, $p<0.001$ to 0.9985, $p<0.0001$) confirmed the strong predictive capability of the models generated through Response Surface Methodology (RSM).

Particle Size

$$= +115.00+2.00A+9.50B-3.50AB-21.00A^2+2.50B^2-9.50A^2B -5.50AB^2 \text{ eqn (1)}$$

Zeta Potential

$$= +0.80 - 4.000E\text{-}003A - 1.000E\text{-}003B - 0.034AB - 0.071A^2 - 0.079B^2 - 0.038A^2B + 0.030AB^2 \text{ eqn (2)}$$

Drug Loading

$$= +24.62-0.19A-0.20B+0.23AB+0.12A^2+ 0.83B^2-0.16A^2B+0.062AB^2 \text{ eqn (3)}$$

Entrapment Efficiency

$$= +77.74+1.03A-0.33B-1.57AB-6.63A^2-2.57B^2- 0.12A^2B+1.85AB^2 \text{ eqn (4)}$$

The results were statistically significant ($p<0.01$) as evaluated by ANOVA using Design Expert® software.

Particle Size

The particle size of the L-Arginine formulations ranged from 89 nm to 128 nm (Table 3 & Figure 3), with the smallest size observed in F10 (89 nm) and the largest in F6 (128±0.44 nm). Smaller particle sizes were achieved with higher polymer concentrations (e.g., 6% Eudragit L100), as seen in F10 (89 nm). Formulations with a lower Solvent: Antisolvent ratio (1:3) produced larger particles, while the 1:5 ratio in F6 led to the largest particle size. The optimized particle size of 114±1.11 nm was achieved in F7,

which had a polymer concentration of 5% and a 1:4 Solvent: Antisolvent ratio.

Zeta Potential

The zeta potential of the L-arginine nanoparticles ranged from 0.637 mV to 0.828 mV (Table 3 & Figure 3), with the highest value observed in batch F7 (0.828 mV). Formulations with a 1:4 solvent-to-antisolvent ratio consistently showed higher zeta potential values (~0.825-0.828 mV), indicating improved colloidal stability. The lowest value (0.637 mV) was recorded in F10, which deviated from the optimal solvent-to-antisolvent ratio.

Entrapment Efficiency

The entrapment efficiency of the L-arginine nanoparticles ranged from 64.54±1.02% (F11) to 77.86±0.93% (F7) (Table 3 & Figure 3). Formulations with 5% Eudragit L100 and a 1:4 solvent-to-antisolvent ratio showed the highest entrapment efficiencies, with F7 reaching 77.86±0.93%. Lower polymer concentrations (4%) and non-optimal solvent ratios (1:3 or 1:5) resulted in reduced entrapment efficiencies, as seen in F11 (64.54±1.02%) and F10 (69.39±0.99%).

Drug Loading

The drug loading of the L-arginine nanoparticles ranged from 24.39±0.17% to 25.98% (Table 3 & Figure 3). The highest drug loading (25.98±0.08%) was observed in F11, although it had lower entrapment efficiency, indicating a trade-off between the two parameters. Formulations with a 1:4 solvent-to-antisolvent ratio showed stable drug loading, confirming that this ratio optimizes drug incorporation without significant loss.

Response surface Methodology

The response surface plot (Figure 4A) demonstrates the effect of Eudragit L100 concentration (A) and Solvent-to-Antisolvent ratio (B) on particle size. An increase in the solvent-to-antisolvent ratio resulted in larger particle sizes, while higher Eudragit L100 concentration initially reduced particle size, with the effect stabilizing at higher concentrations. The smallest particle size (~89 nm) was achieved with a moderate polymer concentration and an optimized solvent-to-antisolvent ratio. The contour plot from Design-Expert® Software also confirms that higher solvent-to-antisolvent ratios lead to larger particle sizes.

The response surface plot (Figure 4B) illustrates the combined effect of Eudragit L100 concentration (X1) and Solvent-to-Antisolvent ratio (X2) on the average zeta potential (Y-axis). The plot reveals a peak region, indicating optimal formulation conditions that result in the highest zeta potential, which suggests maximum colloidal stability. Deviation from this peak-either by changing the Eudragit L100 concentration or the Solvent-to-Antisolvent ratio-causes a decrease in zeta potential, reflecting reduced colloidal stability.

The response surface plot (Figure 4C) demonstrates the impact of Eudragit L100 concentration (A) and Solvent-to-Antisolvent ratio (B) on drug loading (%) in nanoparticles. Higher polymer concentrations and optimized solvent-to-antisolvent ratios led to increased drug loading. The concave surface indicates a nonlinear relationship between the formulation parameters, emphasizing the need for an optimal balance between these variables to maximize drug incorporation. The contour plot further suggests that drug loading progressively increases as the formulation approaches the optimal region.

The response surface plot (Figure 4D) shows the influence of Eudragit L100 concentration (A) and Solvent-to-Antisolvent ratio (B) on entrapment efficiency (%). It indicates that increasing both variables led to higher entrapment efficiency. The curved surface suggests that an optimal balance between polymer concentration and solvent ratio is crucial for maximizing drug entrapment. The contour plot emphasizes the central region with the highest entrapment efficiency, indicating the optimal formulation range.

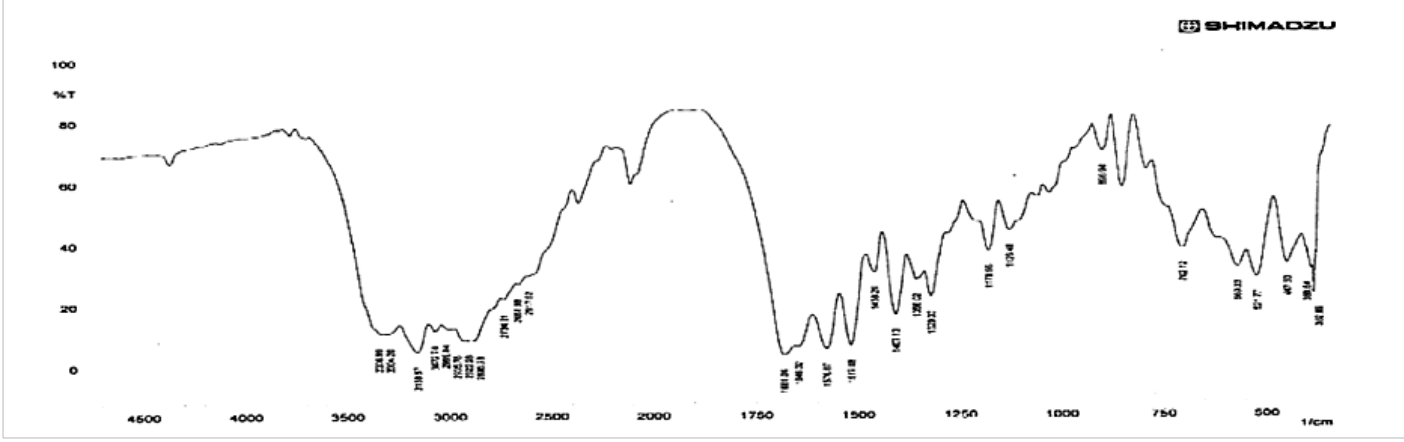

Figure 1: FTIR spectra of L-Arginine.

Table 1: Formulation design for development of Nanoparticles.

Batch Code	Eudragit L 100 (X_1)		Sol: Antisol ratio (X_2)	
	Coded value	Actual Value (mg)	Coded Value	Actual Value
F1	0.00	5	-1.00	1:3
F2	0.00	5	0.00	1:4
F3	0.00	5	0.00	1:4
F4	0.00	5	0.00	1:4
F5	0.00	5	0.00	1:4
F6	0.00	5	1.00	1:5
F7	0.00	5	0.00	1:4
F8	1.00	6	0.00	1:4
F9	-1.00	4	0.00	1:4
F10	1.00	6	1.00	1:5
F11	-1.00	4	-1.00	1:3
F12	1.00	6	-1.00	1:3
F13	-1.00	4	1.00	1:5

Table 2: FTIR characterization of Optimized Nanoparticle.

Functional Group	Characteristic Peak of Pure L-Arginine (cm^{-1})	Characteristic Peak of Formulated Nanoparticles (cm^{-1})	Inference
NH Stretch	3158.57	3156.45	No significant shift, indicating no strong interaction.
CH_3 Stretch	2935.78	2934.12	Minor shift, suggesting stable formulation.
NH_2 Bend	1681.04	1679.85	Negligible shift, confirming structural integrity.
CO Stretch	1576.87	1575.42	Minimal shift, no strong interaction observed.
OH Bend	1517.08	1516.30	No significant change, stable bonding.
CH_3 Asymmetric Bend	1458.25	1457.10	Slight shift, indicating compatibility.
CH_3 Symmetric Bend	1407.13	1406.50	Negligible difference, stable formulation.
CH_3 Symmetric Bend	1356.02	1355.78	No major shift, maintaining structural properties.
OH Bend	1320.33	1319.92	Stable formulation confirmed.
Symmetric Stretch CCC Bond	1176.56	1175.90	No significant interaction observed.
NH_2 Bend	899.46	898.75	Negligible shift, ensuring stability.
CO Bend	521.77	520.88	Minimal change, no strong interaction.
NH_2 Rock	447.50	446.90	Stable peak, confirming formulation integrity.

Table 3: Characterization of formulated nanoparticles.

Batch Code	Particle Size (nm)	Avg Zeta potential (Mv)	Drug Loading (%)	Entrapment Efficiency (%)
F1	109±.1.03	0.658±0.022	25.85±0.12	75.51±1.33
F2	116±0.98	0.825±0.013	24.45±0.18	77.55±1.06
F3	114±0.36	0.827±0.011	24.39±0.17	77.81±0.82
F4	114±1.11	0.826±0.027	24.49±0.21	77.77±0.58
F5	115±0.75	0.825±0.011	24.53±0.06	77.69±0.47
F6	128±0.44	0.656±0.032	25.45±0.21	74.85±0.86
F7	114±0.73	0.828±0.010	24.83±0.15	77.86±0.93
F8	97±0.58	0.661±0.014	24.75±0.19	72.15±0.72
F9	93±0.89	0.669±0.009	25.13±0.07	70.09±1.05
F10	89±1.01	0.637±0.021	25.00±0.22	69.39±0.99
F11	96±0.67	0.662±0.028	25.98±0.08	64.54±1.02
F12	96±0.17	0.782±0.029	25.68±0.11	73.44±.88
F13	103±0.36	0.652±0.036	25.21±0.19	66.78±0.67

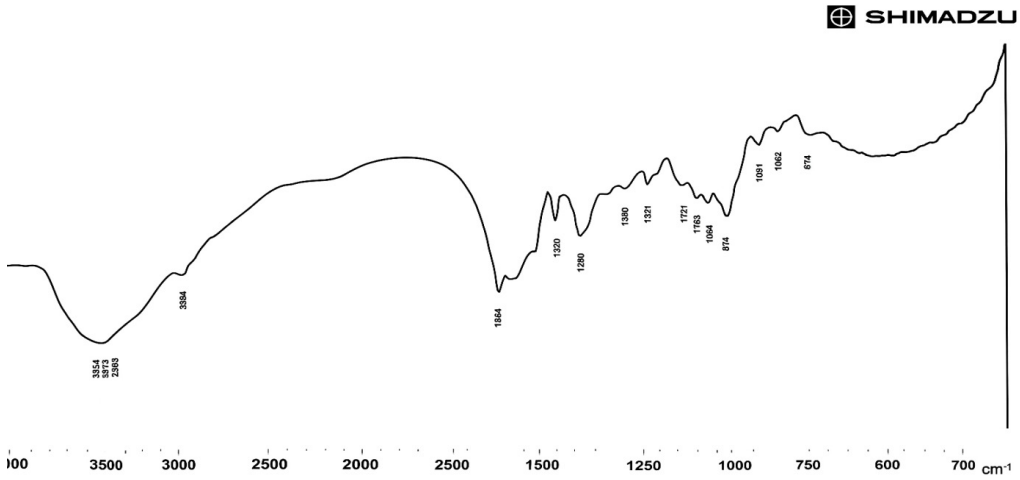

Figure 2: FTIR spectra of L-Arginine Loaded nanoparticles.

Overlay Plot

The overlay plot (Figure 4) demonstrates the combined effects of Eudragit L100 concentration (A) and solvent-to-antisolvent ratio (B) on key formulation parameters, including particle size, zeta potential, drug loading, and entrapment efficiency. It highlights the optimal design space where all responses meet the required criteria, with data labels providing specific values for particle size and zeta potential at selected points.

Validation of optimized formulation batch

The optimized formulations were validated by evaluating their Critical Quality Attributes (CQAs), as detailed in Table 4. A comparison between the observed and predicted responses, generated using Design-Expert® Software, demonstrated a strong correlation. Statistical analysis (Table 4 and Figure 5) indicated high R values (0.964 to 0.999) and a p-value < 0.001, confirming the reliability and accuracy of the model's predictions. Additionally, the overlay plot (Figure 4) further validated the optimized formulation, reinforcing the robustness of the selected conditions.

Surface topography

The SEM image (Figure 6) of L-arginine nanoparticles, prepared using Eudragit L100 via the solvent evaporation method, revealed aggregated clusters with irregular shapes and varying sizes, characteristic of polymeric nanoparticles. The surface appeared porous and rough, indicating efficient solvent evaporation. Although the nanoparticles were in the nanometer range, the observed aggregation could affect dispersibility and potentially influence controlled drug release.

In vitro drug release

The *in vitro* drug release profile (Figure 7) showed a sustained-release pattern for the L-arginine nanoparticles. Initially, there was a slow-release phase (0-2 hr), followed by a rapid increase in drug release between 2-4 hr. After 4 hr, the release rate slowed, reaching a plateau, which indicates controlled drug diffusion. This pattern is typical of sustained-release formulations, where drug release is regulated over a longer period to maintain therapeutic levels.

Drug release kinetics

The drug release kinetics were best described by the Korsmeyer-Peppas model (R^2 = 0.9470, n=0.807), indicating a combination of diffusion and erosion in the release mechanism. The Zero-order model also showed good correlation (R^2=0.9277), suggesting near-constant release, while the Higuchi model indicated diffusion control. The First-order model had the weakest fit, suggesting the release was not purely concentration-dependent.

Stability study of optimized formulations

The stability study showed that key parameters (particle size, zeta potential, drug loading, and entrapment efficiency) remained stable over six months under accelerated conditions (40±2°C, 75±5% RH). The drug release profile at 8 hr also remained unaffected, confirming the formulation's stability (Table 5).

DISCUSSION

The observed melting point of 228°C suggests that the L-Arginine used in the formulation is pure and corresponds well with the reported literature values, affirming the integrity of the compound prior to formulation.

Furthermore, the FTIR analysis revealed that the characteristic functional group peaks remained unaltered in the nanoparticle formulation compared to the pure drug. This indicates that there were no significant chemical interactions between L-Arginine and the polymer used in nanoparticle preparation. The preservation of characteristic peaks in the spectra confirms the compatibility

Table 4: Validation of optimized batch.

Batch code	X1	X2	Response variables	Prediction values	Experimental values	Percentage error
Optimized Batch	-0.66	0.363	Particle Size (nm)	103.97±1.25	103.88±1.18	0.0866
			Zeta Potential	0.7712±0.015	0.7698±0.014	0.1815
			Drug Loading (%)	24.826±0.43	24.836±0.41	-0.0403
			Entrapment Efficiency (%)	74.106±1.02	74.26±1.08	-0.2078
VC1	0.26	-0.47	Particle Size (nm)	110.29±1.36	110.43±1.29	-0.1269
			Zeta Potential	0.7745±0.017	0.7732±0.018	0.1679
			Drug Loading (%)	25.006±0.44	25.106±0.42	-0.3999
			Entrapment Efficiency (%)	76.981±1.11	77.10±1.08	-0.1546
VC2	0.83	-0.46	Particle Size (nm)	101.33±1.21	101.83±1.19	-0.4934
			Zeta Potential	0.7611±0.016	0.7576±0.017	0.4599
			Drug Loading (%)	24.869±0.40	24.961±0.39	-0.3699
			Entrapment Efficiency (%)	74.461±1.03	74.502±1.02	-0.0551
VC3	0.64	-0.77	Particle Size (nm)	104.4±1.30	105.11±1.25	-0.6801
			Zeta Potential	0.762±0.018	0.759±0.017	0.3937
			Drug Loading (%)	25.282±0.41	25.191±0.43	0.3599
			Entrapment Efficiency (%)	75.919±1.06	75.888±1.03	0.0408
VC4	-0.41	-0.48	Particle Size (nm)	107.26±1.32	106.98±1.29	0.2610
			Zeta Potential	0.7656±0.019	0.7639±0.018	0.2220
			Drug Loading (%)	25.019±0.46	25.88±0.44	-3.4414
			Entrapment Efficiency (%)	75.289±1.05	75.201±1.04	0.1169

Table 5: Stability study optimized batch.

Conditions	Duration	Particle Size (nm)	Zeta Potential	Drug Loading (%)	Entrapment Efficiency (%)
Zone II Accelerated (40°C±2°C / 75%RH±5%)	1 month	296.33±2.14	1.634±0.07	96.84±0.13	96.69±0.18
	3 month	296.33±2.10	1.633±0.06	96.83±0.04	96.60±0.09
	6 month	296.32±2.18	1.633±0.08	96.83±0.06	96.60±0.11

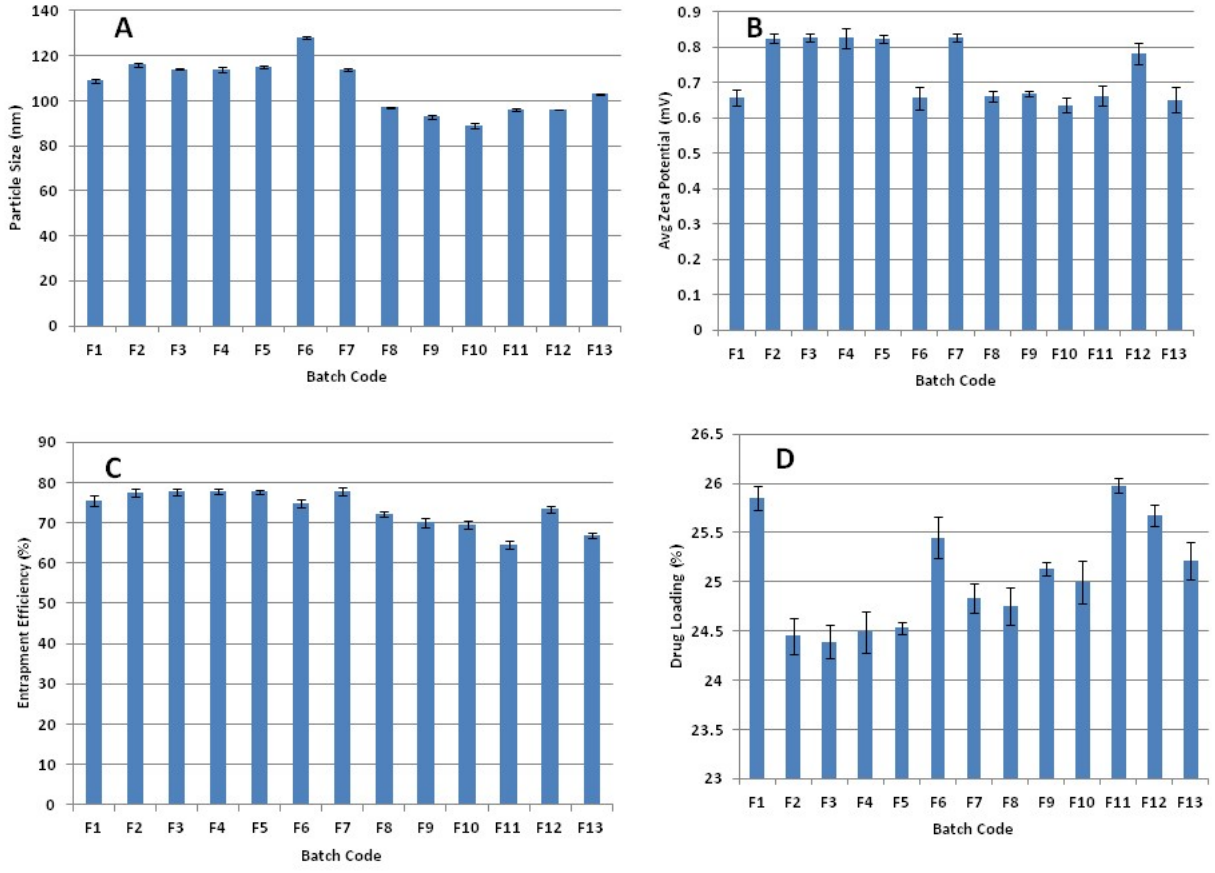

Figure 3: Bar diagram depicting (a) Particle size, (b) Zeta Potential, (c) Entrapement Efficiency and (d) Drug loading (Mean±SD, *n*=3).

of L-Arginine with the chosen polymer, which is crucial for maintaining the drug's stability and therapeutic efficacy in the nanoparticle form.

The 3^2 Central Composite Design (CCD) effectively evaluated the impact of formulation variables on the Critical Quality Attributes (CQAs) of L-Arginine Nanoparticles. Significant R^2 values confirmed the accuracy of the model in predicting outcomes. Particle size was highly influenced by both individual and interactive effects of the variables, with factor A showing strong quadratic effects. Zeta potential demonstrated moderate dependence on the formulation factors. Drug loading was positively affected by the quadratic term of factor B, suggesting optimization of this variable could improve drug incorporation. Entrapment efficiency was sensitive to changes in both interaction and quadratic terms, highlighting the importance of precise formulation control. These results underscore the utility of Response Surface Methodology (RSM) and CCD in optimizing nanoparticulate systems for scale-up and manufacturing.

The particle size of L-arginine nanoparticles was significantly influenced by the polymer concentration and Solvent-to-Antisolvent (S:AS) ratio. Higher Eudragit L100 concentrations (6% in F10 and F8) led to smaller, more uniform particles due to enhanced nucleation and stabilization. The optimal S:AS ratio of 1:4 balanced precipitation, while a higher ratio (1:5 in F6) caused larger particles due to rapid aggregation. Formulation F7 (5% polymer, 1:4 S:AS) achieved a consistent particle size of 114±1.11 nm, ensuring stability for sustained release. These findings

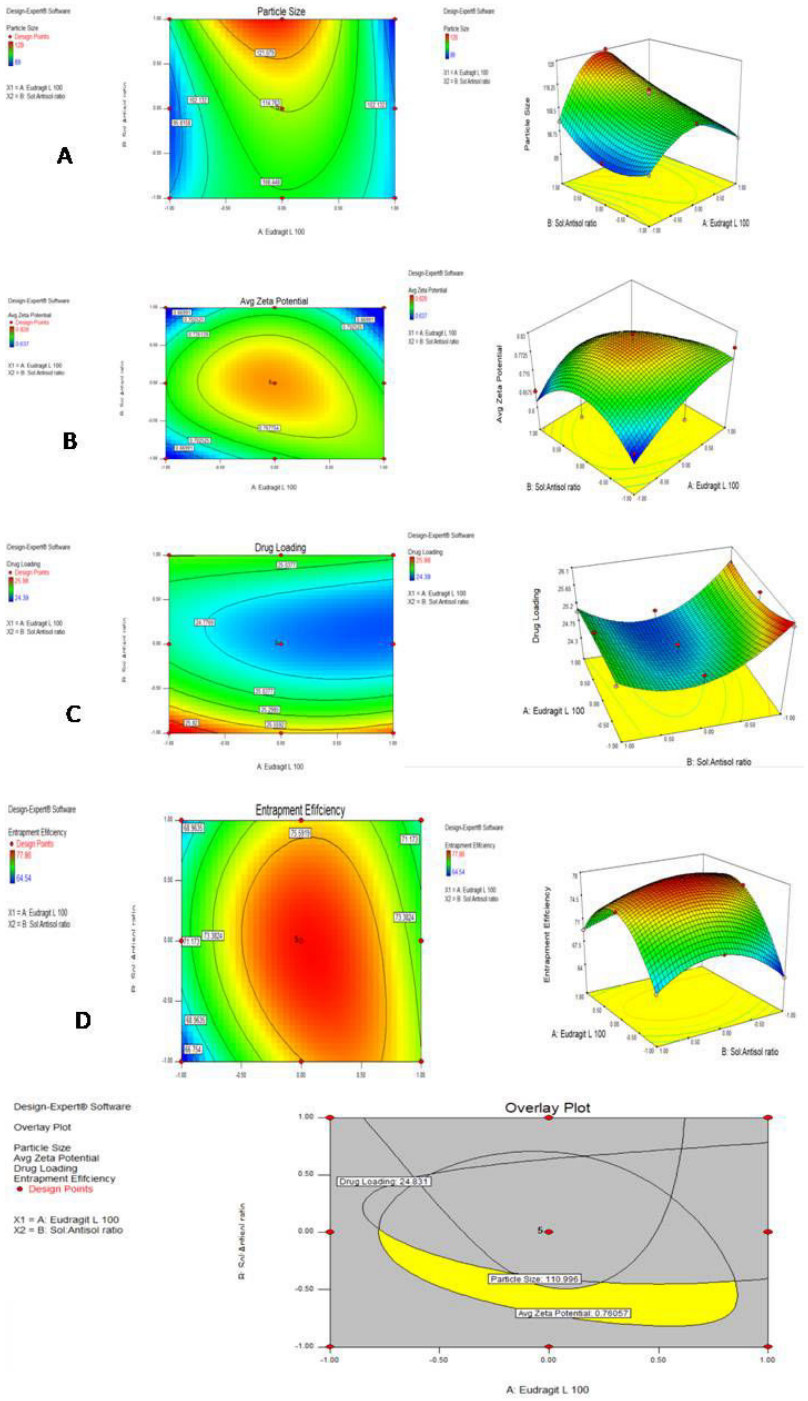

Figure 4: RSM plot and contour plot for Particle size (A); Zeta potential (B); Drug Loading (C) and Entrapment Efficiency (D). and overlay plot.

underscore the importance of carefully controlling formulation parameters for optimal drug delivery.

Particle size of L-arginine nanoparticles was influenced by Eudragit L100 concentration and solvent-to-antisolvent ratio. Higher polymer concentrations (e.g., 6%) resulted in smaller particles, while a 1:4 solvent-to-antisolvent ratio optimized particle size. Excess antisolvent (1:5) caused aggregation and larger particles. The formulation with 5% polymer and a 1:4 ratio (F7) achieved an ideal particle size of 114±1.11 nm, suitable for sustained-release applications. These results highlight the importance of controlling formulation parameters for consistent nanoparticle characteristics.

Entrapment efficiency of L-arginine nanoparticles was influenced by both polymer concentration and solvent-to-antisolvent ratio. The highest entrapment efficiency (77.86±0.93%) was achieved with 5% Eudragit L100 and a 1:4 S:AS ratio (Batch

F7). This optimal combination facilitated the formation of a stable polymer network, enhancing drug encapsulation. Lower polymer concentrations and extreme solvent ratios (1:3 or 1:5) reduced efficiency, likely due to poor matrix formation or premature precipitation. These results highlight the importance of optimizing formulation conditions for improved drug delivery.

Drug loading in L-arginine nanoparticles remained stable across formulations, ranging from 24.39% to 25.98%, indicating consistent drug incorporation. The highest drug loading (25.98%) was observed in F11, but this came with reduced entrapment efficiency, suggesting a trade-off. Formulation F7, which balanced polymer concentration and solvent-to-antisolvent ratio, optimized both parameters. The 1:4 solvent-to-antisolvent ratio proved effective in maintaining drug loading and minimizing loss, ensuring a controlled nanoparticle formation environment. Future efforts should focus on enhancing entrapment efficiency while maintaining optimal drug loading.

The response surface plots for L-arginine nanoparticles highlight that particle size increases with a higher solvent-to-antisolvent ratio, while Eudragit L100 concentration initially decreases particle size, stabilizing at higher concentrations. Zeta potential showed optimal colloidal stability with balanced conditions, while deviations led to aggregation. Drug loading improved with higher polymer concentrations and optimized solvent ratios, requiring careful balance. Entrapment efficiency also increased with higher polymer concentration and solvent ratio, emphasizing the need for precise formulation optimization to achieve stable, high-quality nanoparticles. The overlay plot effectively visualizes the combined effects of Eudragit L100 concentration and solvent-to-antisolvent ratio on key formulation parameters. It identifies regions where formulation adjustments are needed to optimize particle size, stability, and drug encapsulation. The yellow region highlights the optimal conditions, ensuring balanced, efficient nanoparticle properties. The validation of the optimized formulations confirmed the accuracy of Design-Expert® Software in predicting nanoparticle CQAs. Strong linear correlations (R values of 0.964 to 0.999) and low *p*-values (<0.001) demonstrated the model's precision. The overlay plot and brute force method further validated the optimized formulation, ensuring it meets required criteria. These findings provide a solid foundation for future pharmaceutical applications.

SEM analysis showed nanoparticle aggregation, typical in solvent evaporation methods, with irregular shapes and a porous surface. This aggregation may affect dispersibility and controlled release, suggesting that further optimization is needed for improved formulation stability and drug release.

The *in vitro* drug release profile showed sustained-release behavior, with an initial slow release, a rapid phase, and a plateau, indicating controlled drug diffusion. The Korsmeyer-Peppas model best described the release, suggesting both diffusion and erosion control. The Zero-order model supported a constant release rate, ideal for sustained-release systems, while the Higuchi model indicated diffusion control. These findings confirm that the formulation is suitable for controlled drug delivery through a combination of diffusion and erosion mechanisms.

The optimized formulation demonstrated excellent stability, with negligible changes in key parameters over six months. The

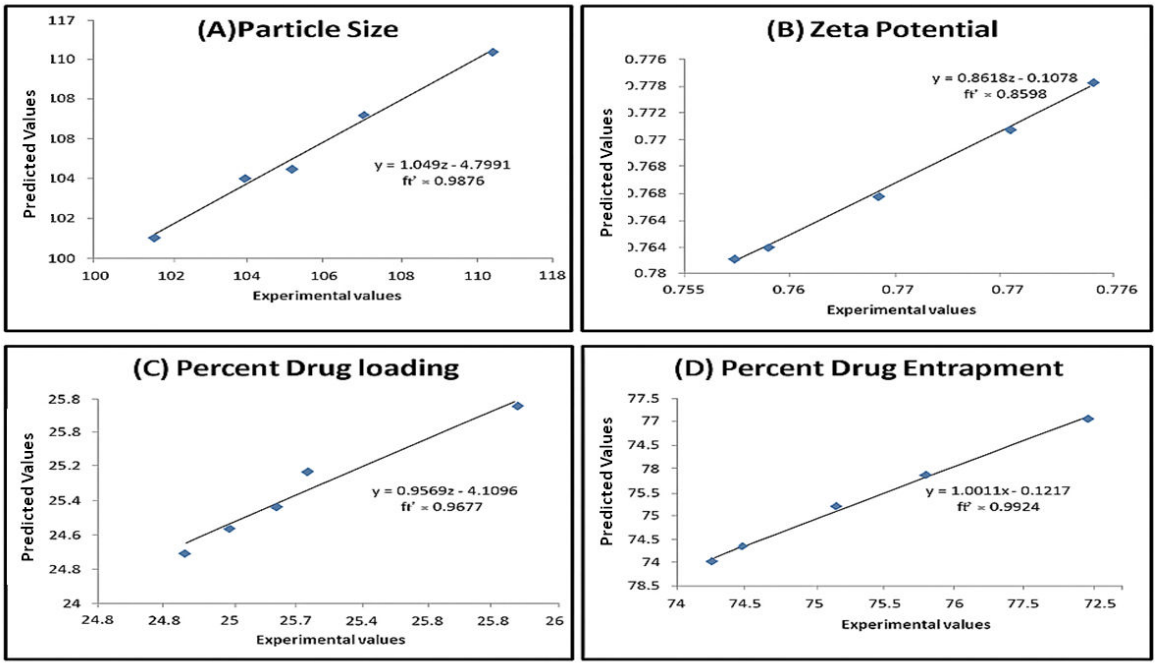

Figure 5: Regression Coefficient between Anticipated and Experimental Response.

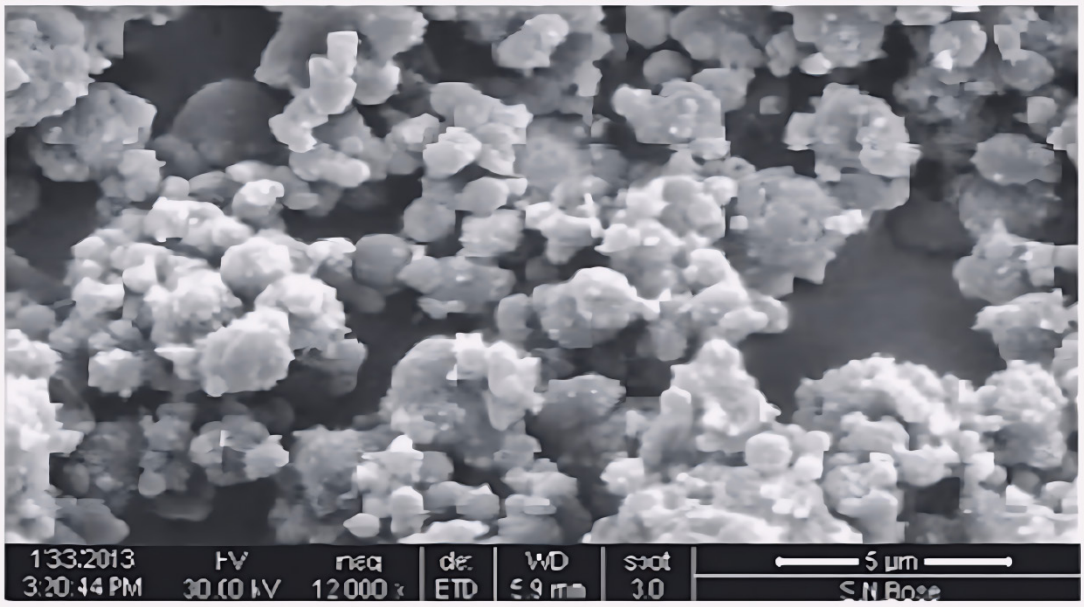

Figure 6: Surface topographic study of optimized batch by SEM.

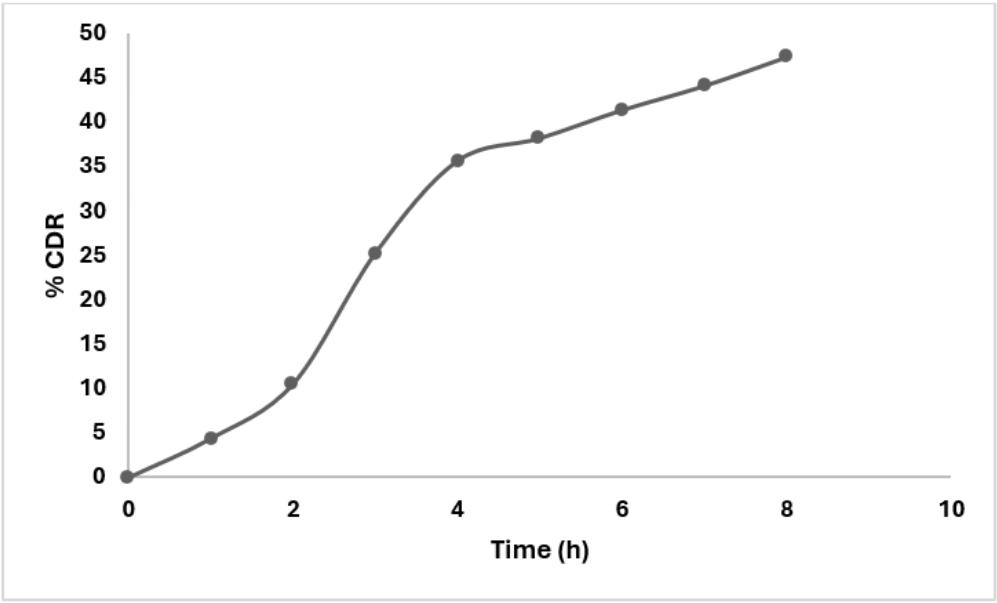

Figure 7: Drug release study from optimized formulation.

consistent drug release profile under accelerated conditions suggests the formulation's robustness and suitability for long-term storage.

CONCLUSION

The study successfully employed the Quality by Design (QbD) approach, utilizing a Face Centered Central Composite Design (FCCCD), to develop and optimize a prolonged-release L-arginine nanoparticle dosage form via the nanoprecipitation technique. The optimized formulation, achieved by controlling the concentration of Eudragit L 100 and the solvent-to-antisolvent ratio, exhibited desirable characteristics: a particle size of 103.97 nm, a zeta potential of 0.771, drug loading of 24.826%, and an entrapment efficiency of 74.26%. Validation of the optimized data demonstrated a close agreement between predicted and experimental values, confirming the robustness and reliability of the developed formulation. Ultimately, this research validates the efficiency of the QbD methodology in rationalizing the optimization of complex L-arginine drug delivery systems, minimizing extensive experimentation while ensuring high-quality, controlled-release nutraceutical formulations.

ACKNOWLEDGEMENT

None.

ABBREVIATIONS

FCCCD: Face-Centered Central Composite Design; **UV:** Ultraviolet-Visible, **HPLC:** High-Performance Liquid Chromatography, **FTIR:** Fourier Transform Infrared Spectroscopy, **SEM:** Scanning electron Microscopy, **MLRA:** Multiple Linear Regression Analysis, **CQA:** Critical Quality Attributes, **CMA:** Critical Material Attributes.

CONFLICT OF INTEREST

The authors declare that there is no conflict of interest.

AUTHOR CONTRIBUTION

Dr. Vijay Sharma as main author conceptualized and supervised the study; designed the experiments and optimized the formulation and performed data analysis and interpretation;. Vijay Sharma, Mr. Maneesh Kumar and Mr. Gurvinder Pal Singh conducted the laboratory experiments and prepared the manuscript draft; and Dr. Gyanendra Kumar Singh and Dr. Navneet Verma reviewed, edited, and finalized the manuscript for submission.

REFERENCES

Beck-Broichsitter, M., Rytting, E., Lebhardt, T., Wang, X., and Kissel, T. (2010). Preparation of nanoparticles by solvent displacement for drug delivery: A shift in the "ouzo region" upon drug loading. *European Journal of Pharmaceutical Sciences, 41*(2), 244-253.

Becker, Y., Olshevsky, U., and Levitt, J. (1967). The role of arginine in the replication of herpes simplex virus. *Journal of General Virology, 1*, 471-478.

Bhalani, D. V., Nutan, B., Kumar, A., and Singh Chandel, A. K. (2022). Bioavailability enhancement techniques for poorly aqueous soluble drugs and therapeutics. *Biomedicines, 10*(9), 2055. https://doi.org/10.3390/biomedicines10092055

Carissimi, G., Montalbán, M. G., Víllora, G., and Barth, A. (2020). Direct quantification of drug loading content in polymeric nanoparticles by infrared spectroscopy. *Pharmaceutics, 12*(10), 912. https://doi.org/10.3390/pharmaceutics12100912

Goldstein, A., Soroka, Y., Frušić-Zlotkin, M., Popov, I., and Kohen, R. (2014). High resolution SEM imaging of gold nanoparticles in cells and tissues. *Journal of Microscopy, 256*(3), 237-247. https://doi.org/10.1111/jmi.12179

Hanif, M., Khan, H. U., Maheen, S., Shafqat, S. S., Shah, S., Masood, S. A., Abbas, G., Rizwan, M., Rasheed, T., and Bilal, M. (2021). Formulation, characterization, and pharmacokinetic evaluation of Ivabradine-Nebivolol co-encapsulated lipospheres. *Journal of Molecular Liquids, 344*, 117704. https://doi.org/10.1016/j.molliq.2021.117704

López-Ruiz, M., Navas, F., Fernández-García, P., Martínez-Erro, S., Fuentes, M. V., Giráldez, I., Ceballos, L., Ferrer-Luque, C. M., Ruiz-Linares, M., Morales, V., Sanz, R., and García-Muñoz, R. A. (2022). L-arginine-containing mesoporous silica nanoparticles embedded in dental adhesive (Arg@MSN@DAdh) for targeting cariogenic bacteria. *Journal of Nanobiotechnology, 20*(1), 502. https://doi.org/10.1186/s12951-022-01714-0

Mast, M. P., Modh, H., Knoll, J., Fecioru, E., and Wacker, M. G. (2021). An update to dialysis-based drug release testing—Data analysis and validation using the Pharma Test Dispersion Releaser. *Pharmaceutics, 13*(12), 2007. https://doi.org/10.3390/pharmaceutics13122007

Rizvi, S. A. A., and Saleh, A. M. (2018). Applications of nanoparticle systems in drug delivery technology. *Saudi Pharmaceutical Journal, 26*(1), 64-70. https://doi.org/10.1016/j.jsps.2017.10.012

Sadhukhan, B., Mondal, N. K., and Chattoraj, S. (2016). Optimisation using central composite design (CCD) and the desirability function for sorption of methylene blue from aqueous solution onto *Lemna major*. *Karbala International Journal of Modern Science, 2*(3), 145-155. https://doi.org/10.1016/j.kijoms.2016.03.005

Salatin, S., Barar, J., Barzegar-Jalali, M., Adibkia, K., Kiafar, F., and Jelvehgari, M. (2017). Development of a nanoprecipitation method for the entrapment of a very water soluble drug into Eudragit RL nanoparticles. *Research in Pharmaceutical Sciences, 12*(1), 1-14. https://doi.org/10.4103/1735-5362.199041

Stetefeld, J., McKenna, S. A., and Patel, T. R. (2016). Dynamic light scattering: A practical guide and applications in biomedical sciences. *Biophysical Reviews, 8*(4), 409-427. https://doi.org/10.1007/s12551-016-0218-6.

Tian, S., Li, J., Tao, Q., Zhao, Y., Lv, Z., Yang, F., Duan, H., Chen, Y., Zhou, Q., and Hou, D. (2018). Controlled drug delivery for glaucoma therapy using montmorillonite/Eudragit microspheres as an ion-exchange carrier. *International Journal of Nanomedicine, 13*, 415-428. https://doi.org/10.2147/IJN.S146346

Wu, G., Bazer, F. W., Davis, T. A., Kim, S. W., Li, P., Rhoads, J. M., Satterfield, M. C., Smith, S. B., Spencer, T. E., and Yin, Y. (2009). Arginine metabolism and nutrition in growth, health and disease. *Amino Acids, 37*(1), 153-168. https://doi.org/10.1007/s00726-008-0210-y

Cite this article: Sharma V, Singh MK, Singh GP, Sharma GK, Verma N. Design and Optimization of Arginine-Loaded Nutraceutical Nanoparticles via Face-Centered Central Composite Approach. Int. J. Pharm. Investigation. 2026;16(3):1123-34.